J Mater Sci (2008) 43:7366–7371
DOI 10.1007/s10853-008-2846-0

ULTRAFINE-GRAINED MATERIALS

Developing superplasticity in a magnesium AZ31 alloy by ECAP

Roberto B. Figueiredo · Terence G. Langdon

Received: 14 February 2008 / Accepted: 30 June 2008 / Published online: 26 July 2008

Abstract The processing of a magnesium AZ31 alloy by equal-channel angular pressing refines the grain size to ~2.2 μm, but annealing for 30 min at 673 K coarsens the grains to ~6.0 μm. Despite this microstructural instability, the alloy is superplastic when pulled in tension at temperatures in the range of 623–723 K with elongations up to >1000% at strain rates at and below 10^{-4} s^{-1}. Experiments within the superplastic regime show the strain rate sensitivity is ~0.5 and the activation energy is close to the value for grain boundary diffusion. It is demonstrated by calculation that the experimental results are in good agreement with a model for superplasticity based on grain boundary sliding.

Introduction

It is now recognized that equal-channel angular pressing (ECAP) provides a powerful tool for introducing significant grain refinement into bulk metallic materials so that the processed grain sizes are typically within the submicrometer range [1]. Since superplasticity is dependent upon the presence of small grain sizes, usually <10 μm [2], it is apparent that processing by ECAP may provide an opportunity for achieving superplastic behavior at elevated temperatures [3, 4]. Defining superplasticity as elongations at or above 500%, a recent review recorded a large number of materials, including numerous aluminum and magnesium alloys, where superplastic capabilities were attained after processing by ECAP [5].

An examination of the published data for magnesium shows reports of exceptionally high elongations of 1780% in a Mg–8% Li alloy [6] and 2040% in a ZK60 (Mg–4.9% Zn–0.7% Zr) alloy [7, 8] where all compositions are given in weight percent. Very recently an even higher elongation of 3050% was reported for a ZK60 alloy after ECAP where this represents the highest superplastic elongation achieved in any magnesium alloy processed under any conditions with or without ECAP [9]. There are also several reports of superplasticity after ECAP in the AZ-series of magnesium alloys which are rich in aluminum and zinc including elongations of 1320% in the AZ61 (Mg–6% Al–1% Zn) alloy [10] and 956% in the AZ91 (Mg–9% Al–1% Zn) alloy [11].

Despite these successes, there are no reports to date of the occurrence of superplasticity in the AZ31 (Mg–3% Al–1% Zn) alloy. For example, Lin et al. [12] investigated the mechanical properties of the AZ31 alloy processed by ECAP and obtained a maximum elongation of 460% at 423 K but, in addition, reported lower elongations at higher temperatures because of the occurrence of grain growth. Watanabe et al. [13] processed an AZ31 alloy by ECAP and then annealed at 673 K, but superplastic elongations were not attained at either 573 or 673 K. These preliminary results suggest that the use of ECAP as a processing tool to produce a superplastic capability may be ineffective in the AZ31 alloy due to an inherent lack of microstructural stability at elevated temperatures. Accordingly, the present investigation was initiated to evaluate the potential for achieving superplastic elongations in the AZ31 alloy after processing by ECAP and to examine the nature of the flow behavior at high temperatures.

R. B. Figueiredo (✉) · T. G. Langdon
Departments of Aerospace & Mechanical Engineering and Materials Science, University of Southern California, Los Angeles, CA 90089-1453, USA
e-mail: figueire@usc.edu

T. G. Langdon
Materials Research Group, School of Engineering Sciences, University of Southampton, Southampton SO17 1BJ, UK

Experimental material and procedures

The AZ31 (Mg–3% Al–1% Zn) alloy was provided by Timminco Corporation (Aurora, CO) in the form of extruded rods with diameters of 10 mm. Billets having lengths of 60 mm were cut and used for processing through an ECAP die having an internal angle, Φ, of 110° between the two channels and an external arc of curvature, Ψ, of 20°. It is known that this geometry imposes a strain of $\sim$0.8 on each separate pass through the die [14]. Billets were pressed through four passes at either 453 or 473 K using processing route B_C in which the billets were rotated in the same sense by 90° about the longitudinal axis between each pass [15]. Tensile specimens were machined from the billets both before and after ECAP with the gauge lengths of 4 mm lying parallel to the longitudinal axes and with cross-sectional areas of 2×3 mm^2. These specimens were pulled to failure in the temperature range from 623 to 723 K using an Instron testing machine operating at a constant rate of cross-head displacement and with initial strain rates from $\sim 10^{-5}$ to $\sim 10^{-1}$ s^{-1}. The cross-head displacement rates were varied in the initial stages of some of the tests to determine the evolution of load under different strain rates. All load and displacement data were converted to provide plots of the true stress as a function of the true strain. The stress–strain curves were plotted at the different strain rates and for each specimen the flow stress was taken as the value of stress at a strain of 0.1. All the elongations to failure were determined by excluding any additional deformation that may occur in the grip sections at either end of the tensile specimens.

For metallographic analysis, samples were cut from billets in the as-received condition, immediately following ECAP processing and after processing by ECAP and annealing at 673 K for 30 min. Each sample was ground with SiC papers followed by a final polishing with 0.05 μm alumina powder. An etching solution, acetic-picral (70 mL ethanol, 4.2 g picric acid, 10 mL acetic acid, 10 mL water), was used to reveal the grain structure of the samples using optical microscopy. Following conventional practice in ECAP processing, the experimental grain sizes quoted in this report correspond to the mean linear intercept grain size, d, determined from measurements taken along linear traverses. For the calculation of the superplastic flow rate, the mean linear intercept grain size was converted to the spatial grain size, d_s, using the relationship $d_s = 1.74 \times d$.

Experimental results

Representative microstructures are given in Fig. 1 for four different conditions: (a) shows the as-received alloy with an average linear intercept grain size of $\sim$9.1 μm, (b) shows the structure after annealing the as-received material for 30 min at 673 K where there is a slight increase in the average grain size to $\sim$10.2 μm and (c) shows the microstructure after pressing through four passes at 473 K where the grain size has been refined to $\sim$2.2 μm and

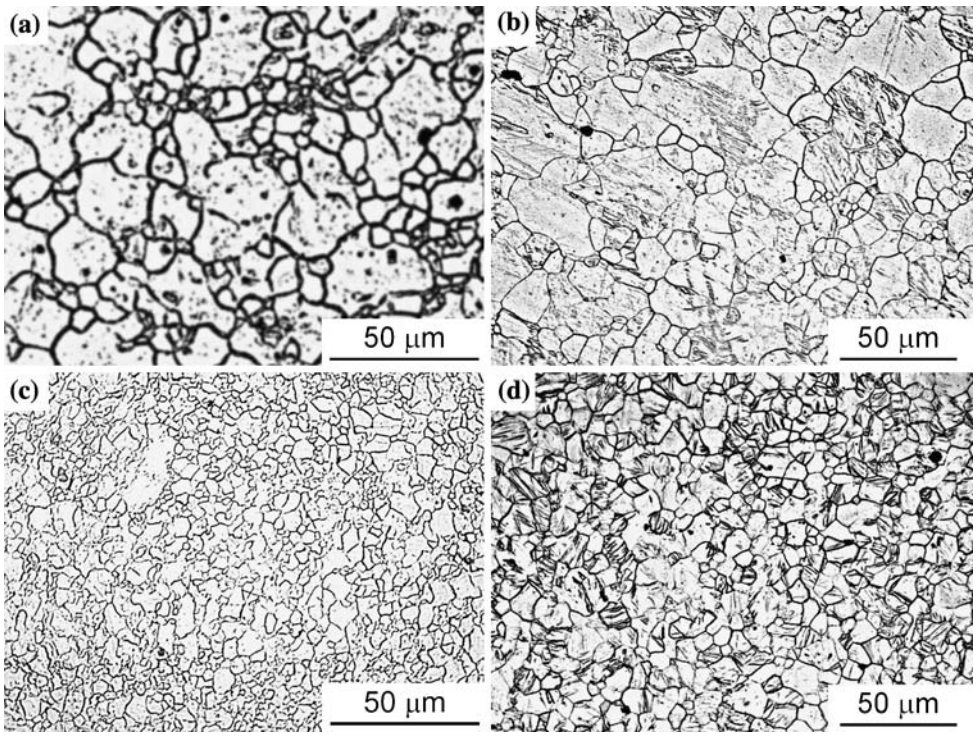

Fig. 1 Grain structure of the AZ31 alloy (**a**) in the as-received condition, (**b**) after 30 min annealing at 673 K, (**c**) after four passes of ECAP at 473 K, (**d**) after ECAP processing and annealing

(d) shows the effect of annealing the pressed material for 30 min at 673 K to give a grain size of ~6.0 μm. The measured grain size after pressing for four passes at the lower temperature of 453 K was identical to the grain size recorded after pressing at 473 K. After additional annealing for 30 min at 673 K, the material pressed at 453 K had a measured grain size of ~5.9 μm.

Figure 2 shows examples of the true stress–true strain curves for tests conducted at different strain rates at 723 K for the alloy processed by ECAP at 473 K. The flow stress was determined at a strain of 0.1 for the different strain rates using the extrapolated trend lines. The strain rate change tests demonstrate a general consistency between the levels of stress recorded at the different strains. The values of the flow stress, σ, normalized by the shear modulus, G, are plotted in Fig. 3 as a function of the initial strain rate, $\dot{\varepsilon}$, for three different material conditions: (a) for the as-received condition, (b) for the samples pressed at 453 K and (c) for the samples pressed at 473 K, where datum points are shown for different testing temperatures: the value of G was taken as $G = (1.92 \times 10^4 - 8.6\,T)$ MPa, where T is the absolute temperature [16]. These plots show the anticipated displacement to faster strain rates as the grain size is reduced, thereby confirming the occurrence of a grain boundary flow process. There is also a trend towards a strain rate sensitivity of $m \approx 0.5$ in all three conditions at the lower strain rates.

Each sample was pulled to failure and Fig. 4 shows the measured elongations to failure plotted against the initial strain rate. Although the results are scattered, three trends are visible. First, the elongations tend to increase with decreasing strain rate such that superplastic ductilities are achieved at strain rates at and below $\sim 10^{-3}$ s^{-1} in the samples processed by ECAP with maximum elongations of more than 1000% at and below 10^{-4} s^{-1}. Second, the

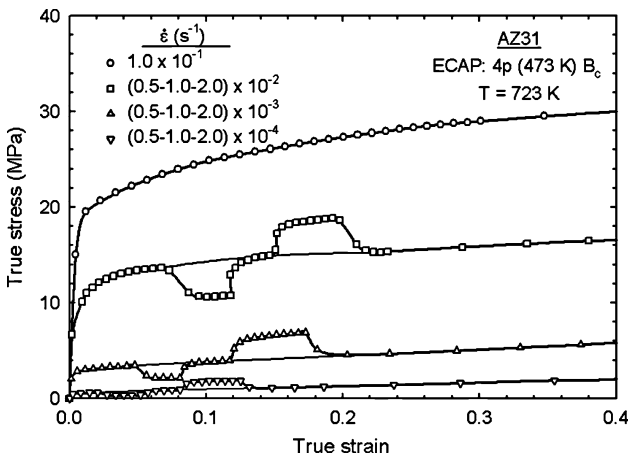

Fig. 2 True stress–true strain curves for the alloy processed by four passes of ECAP at 473 K and tested at 723 K with changes in the strain rate in the initial stage of the tests

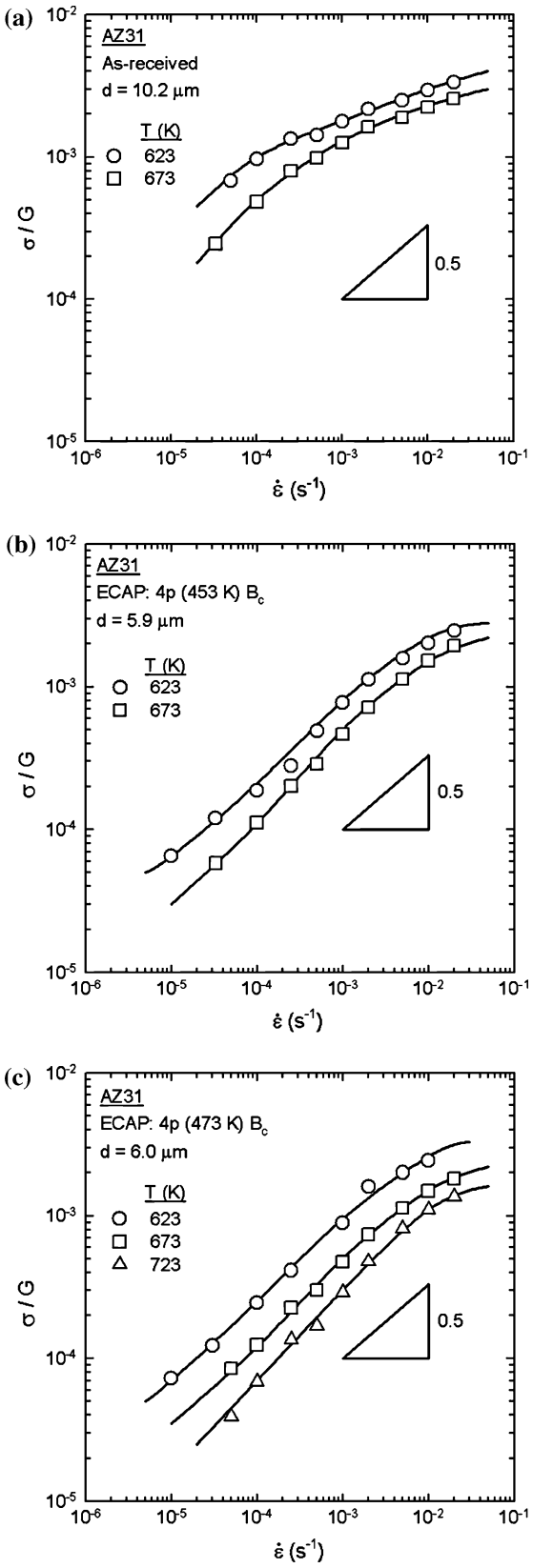

Fig. 3 Normalized stress as a function of the strain rate for (**a**) the as-received AZ31 alloy, (**b**) after 4 passes of ECAP at 453 K, (**c**) after four passes of ECAP at 473 K

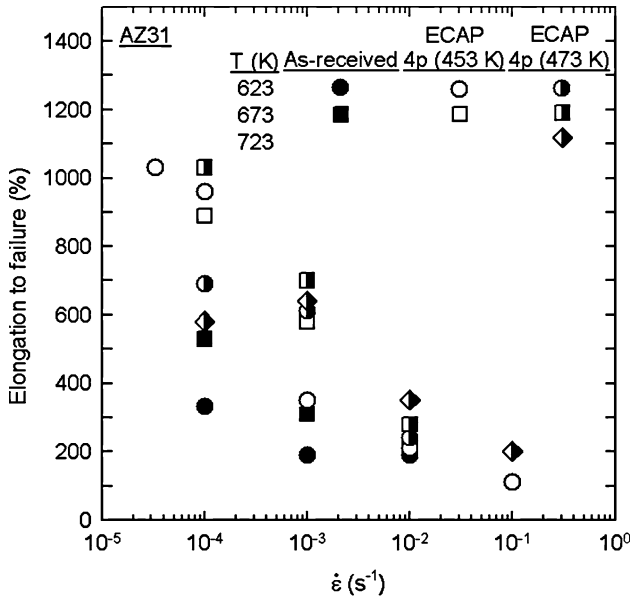

Fig. 4 Elongation to failure as a function of strain rate for the AZ31 alloy before and after ECAP for tests at different temperatures

measured elongations after processing by ECAP are consistently higher than in the as-received material where the grain size is larger. Third, there is no significant difference, at least within the scatter in the datum points, between the measured elongations after ECAP at 453 and 473 K.

Discussion

Effect of ECAP on grain structure and superplastic elongation

These results show that processing by ECAP refines the grain structure of the extruded AZ31 alloy. The degree of refinement was not sufficient to produce an ultrafine-grained structure with an average grain size of <1 μm, but nevertheless the measured grain size of ~2.2 μm after ECAP is within the range of other reports describing the application of ECAP to the AZ31 alloy. Thus, earlier reports gave grain sizes after ECAP of ~0.7 μm [12], ~1.29 μm [17], ~1.4 μm [18], ~2.5 μm [19], ~3 μm [20] and in the range of ~1–3 μm [21, 22]. Although there is evidence that a reduction in the processing temperature reduces the grain size in ECAP [18, 20], the processing temperatures were probably too close to reveal this trend in the present experiments. There are small differences in the measured elongations recorded in Fig. 4 for the samples pressed at the two different temperatures, but nevertheless the curves of flow stress against strain rate for these two samples, shown in Fig. 3b, c, are very consistent and almost identical.

Annealing tests show the fine microstructure is not stable at high temperatures and the grain size increased after annealing for 30 min at 673 K by almost a factor of 3× to an average size of ~6.0 μm. Although this demonstrates significant structural coarsening at high temperatures, the final grain size recorded in this investigation was significantly smaller than the spatial grain size of ~18 μm, equivalent to a linear intercept grain size of ~10.3 μm, recorded earlier in an AZ31 alloy processed by ECAP and annealed under the same conditions of 30 min at 673 K [13].

The results provide a clear demonstration that processing by ECAP improves the ductility of the as-received AZ31 alloy. Excellent superplastic elongations from 500% to more than 1000% were observed in samples processed by ECAP and tested at strain rates at and below 10^{-3} s^{-1} whereas in the as-received condition the measured elongations were almost consistently below 500%.

An analysis of the superplastic flow behavior

The relation between flow stress and strain rate determined by the experiments allows an evaluation of the flow behavior of the AZ31 alloy. The steady-state strain rate in high temperature flow is given by a relationship of the form

$$\dot{\varepsilon} = \frac{ADGb}{kT}\left(\frac{\mathbf{b}}{d_s}\right)^p \left(\frac{\sigma}{G}\right)^n \quad (1)$$

where A is a dimensionless constant, D is the diffusion coefficient, $\mathbf{b}$ is the Burgers vector, k is Boltzmann's constant, d_s is the spatial grain size, p is the exponent of the inverse grain size and n is the stress exponent. The values of the constant A, the activation energy incorporated into the diffusion coefficient and the exponents p and n serve to differentiate between different flow mechanisms.

Superplasticity occurs through the process of grain boundary sliding in which individual grains are displaced with respect to each other within the bulk polycrystalline solid [23]. It is now well established that the superplastic flow mechanism is based on the movement of dislocations along the grain boundaries with some limited intragranular slip acting as an accommodation process. This type of behavior is consistent with experimental results [24] and the strain rate is then given by Eq. 1 with $A \approx 10$, the diffusion coefficient for grain boundary diffusion, D_{gb}, and exponents for the inverse grain size and the stress of $p = 2$ and $n = 2$, respectively [25].

The inverse of the stress exponent is equivalent to the strain rate sensitivity, m, and this is given by the slope of a logarithmic plot of σ/G against strain rate as shown in Fig. 3. These results show that $m \approx 0.5$, equivalent to $n \approx 2$, for the samples pressed at the two different

temperatures at strain rates corresponding to those recorded in Fig. 4 where the alloy is superplastic. There is also evidence for a transition to a higher value of m for the as-received material at the very lowest strain rates below $\sim 10^{-4}$ s^{-1} but the elongations were not measured in this very low range.

The coefficient for grain boundary diffusion, D_{gb}, may be represented by a relationship of the form

$$\delta D_{gb} = \delta D_0 \exp\left(\frac{-Q_{gb}}{RT}\right) \quad (2)$$

where δ is the grain boundary width, D_0 is the pre-exponential frequency factor, Q_{gb} is the activation energy for grain boundary diffusion and R is the gas constant.

The experimental activation energy for flow can be determined by plotting the temperature-compensated strain rate against the reciprocal of the absolute temperature for a selected value of σ/G. This result is shown in Fig. 5 using a value of $\sigma/G = 2 \times 10^{-4}$ and taking $n = 2$ for the material processed by ECAP at 473 K where tests were conducted at three different temperatures. From this plot, the activation energy is estimated as $Q \approx 84$ kJ mol^{-1} where this value is very close to the anticipated activation energy of 92 kJ mol^{-1} reported for grain boundary diffusion in magnesium [26]. Thus, this result is consistent with the expectations of flow occurring by the conventional mechanism developed for superplasticity controlled by grain boundary sliding.

It is possible to make a direct comparison with the theoretical mechanism for superplasticity by taking $\delta D_0 = 5.0 \times 10^{-12}$ m^3 s^{-1} and $Q_{gb} = 92$ kJ mol^{-1} for

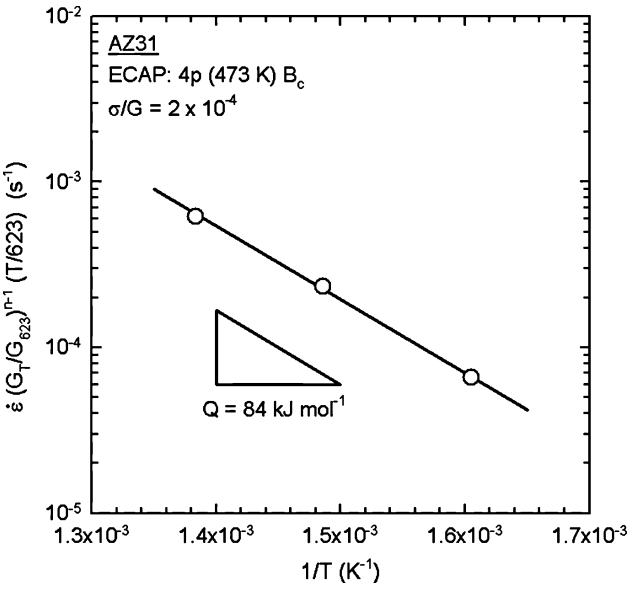

Fig. 5 Semi-logarithmic plot of the strain rate as a function of the inverse of the temperature showing the experimental activation energy

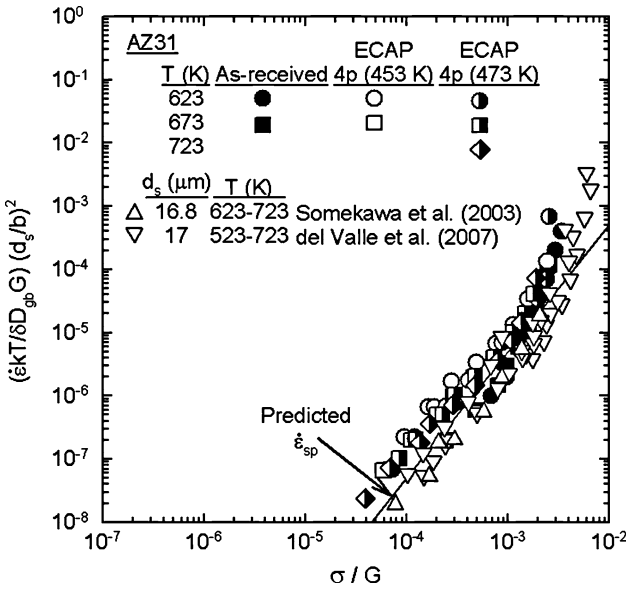

Fig. 6 Normalized strain rate versus normalized stress including the theoretical prediction for superplastic flow [25] and data from Somekawa et al. [27] and del Valle et al. [28]

grain boundary diffusion in magnesium [26], a grain boundary width of $\delta = 2b$ where $b = 3.2 \times 10^{-10}$ m for magnesium [16], and using Eq. 1 with $n = 2$ and $p = 2$. The result is shown in Fig. 6 where the strain rate is plotted in a normalized form to incorporate the differences in temperature and grain size. The theoretical strain rate for superplasticity, $\dot{\varepsilon}_{sp}$, is given by the solid line [25] and the various experimental datum points are taken from the present experiments using both the as-received and the ECAP materials and, in addition, datum points taken from earlier experiments on two fine-grained AZ31 alloys produced without processing by ECAP by Somekawa et al. [27] and del Valle et al. [28]. For the latter results, Fig. 6 indicates the values of the spatial grain size, d_s, in each experiment.

Inspection of Fig. 6 shows excellent agreement with the theoretical model for superplasticity for all experiments over a range of normalized stresses in the vicinity of $\sigma/G \approx 10^{-4}$–10^{-3} but with a tendency to deviate to more rapid strain rates at normalized stresses above $\sim 10^{-3}$. It is apparent that all the experimental points within the superplastic region are in agreement with the theoretical model to within approximately one order of magnitude on the normalized strain rate axis. The transition at the higher stresses corresponds to the conventional transition with increasing stress from superplastic flow with $n = 2$ to control by an intragranular dislocation mechanism with $n > 2$ [29].

There is an excellent consistency in Fig. 6 between the present results obtained on AZ31 either tested in the as-received and extruded condition or tested after

processing by ECAP and the two sets of additional data taken from other reports on the same alloy. Somekawa et al. [27] used rolled AZ31; they conducted an annealing treatment similar to the present work and obtained an average spatial grain size of 16.8 μm. In the experiments of del Valle et al. [28], an AZ31 alloy was processed by rolling and annealing to give an average grain size of 17 μm. The agreement between all sets of data in Fig. 6 confirms that the model accurately predicts the behavior of fine-grained AZ31 alloy independent of whether the alloy is processed by rolling, extrusion or ECAP. It is important also to note that the grain size of the ECAP material was smaller than the extruded or rolled materials and this led to the higher superplastic elongations after processing by ECAP. Thus, the highest recorded elongations in these experiments were ~1000% after ECAP processing with a grain size of 2.2 μm, ~500% in the as-received extruded condition, ~404% in experiments on rolled AZ31 with a grain size of 17 μm [27], and although the values of the elongations were not directly reported by del Valle et al. [28], an earlier report from this group gave a maximum elongation of ~320% for rolled AZ31 [30].

Conclusions

(1) Extruded billets of the magnesium AZ31 alloy were processed by ECAP to refine the structure to an average grain size of ~2.2 μm. Annealing for 30 min at 673 K after ECAP gave some grain coarsening to ~6.0 μm.

(2) Superplastic elongations were recorded after ECAP processing when testing in the temperature range from 623 to 723 K at strain rates at and below 10^{-3} s^{-1}. Very high elongations up to >1000% were obtained at strain rates at and below 10^{-4} s^{-1}.

(3) Within the superplastic regime the strain rate sensitivity was ~0.5 and the activation energy was close to the value anticipated for grain boundary diffusion. The results showed good agreement with a theoretical model for superplasticity controlled by grain boundary sliding.

Acknowledgements One of the authors (RBF) was supported by a CAPES/Fulbright Scholarship. This work was supported by the U.S. Army Research Office under Grant No. W911NF-05-1-0046.

References

1. Valiev RZ, Langdon TG (2006) Prog Mater Sci 51:881. doi:10.1016/j.pmatsci.2006.02.003
2. Langdon TG (1982) Metall Trans 13A:689
3. Xu C, Horita Z, Furukawa M, Langdon TG (2004) J Mater Eng Perform 13:683. doi:10.1361/10599490421385
4. Kawasaki M, Figueiredo RB, Xu C, Langdon TG (2007) Metall Mater Trans 38A:1891
5. Kawasaki M, Langdon TG (2007) J Mater Sci 42:1782. doi:10.1007/s10853-006-0954-2
6. Furui M, Kitamura H, Anada H, Langdon TG (2007) Acta Mater 55:1083. doi:10.1016/j.actamat.2006.09.027
7. Lapovok R, Cottam R, Thomson PF, Estrin Y (2005) J Mater Res 20:1375. doi:10.1557/JMR.2005.0180
8. Lapovok R, Thomson PF, Cottam R, Estrin Y (2005) Mater Sci Eng A 410–411:390. doi:10.1016/j.msea.2005.08.067
9. Figueiredo RB, Langdon TG (2008) Adv Eng Mater 10:37. doi:10.1002/adem.200700315
10. Myahara Y, Horita Z, Langdon TG (2006) Mater Sci Eng A 420:240. doi:10.1016/j.msea.2006.01.043
11. Mabuchi M, Ameyama K, Iwasaki H, Higashi K (1999) Acta Mater 47:2047. doi:10.1016/S1359-6454(99)00094-4
12. Lin HK, Huang JC, Langdon TG (2005) Mater Sci Eng A 402:250. doi:10.1016/j.msea.2005.04.018
13. Watanabe H, Takara A, Somekawa H, Mukai T, Higashi K (2005) Scr Mater 52:449. doi:10.1016/j.scriptamat.2004.11.011
14. Iwahashi Y, Wang J, Horita Z, Nemoto M, Langdon TG (1996) Scr Mater 35:143. doi:10.1016/1359-6462(96)00107-8
15. Furukawa M, Iwahashi Y, Horita Z, Nemoto M, Langdon TG (1998) Mater Sci Eng A 257:328. doi:10.1016/S0921-5093(98)00750-3
16. Vagarali SS, Langdon TG (1982) Acta Metall 30:1157. doi:10.1016/0001-6160(82)90009-8
17. Jin L, Dongliang L, Mao D, Zeng X, Ding W (2006) J Alloy Comp 426:148. doi:10.1016/j.jallcom.2006.02.018
18. Su CW, Lu L, Lai MO (2006) Mater Sci Eng A 434:227. doi:10.1016/j.msea.2006.06.103
19. Kim HK, Kim WJ (2004) Mater Sci Eng A 385:300
20. Xia K, Wang JT, Wu X, Chen G, Gurvan M (2005) Mater Sci Eng A 410–411:324. doi:10.1016/j.msea.2005.08.123
21. Zuberová Z, Estrin Y, Lamark TT, Janecek M, Hellmig RJ, Krieger M (2007) J Mater Proc Tech 184:294. doi:10.1016/j.jmatprotec.2006.11.098
22. Janecek M, Popov M, Krieger MG, Hellmig RJ, Estrin Y (2007) Mater Sci Eng A 462:116. doi:10.1016/j.msea.2006.01.174
23. Langdon TG (1994) Mater Sci Eng A 174:225. doi:10.1016/0921-5093(94)91092-8
24. Valiev RZ, Langdon TG (1993) Acta Metall Mater 41:949. doi:10.1016/0956-7151(93)90029-R
25. Langdon TG (1994) Acta Metall Mater 42:2437. doi:10.1016/0956-7151(94)90322-0
26. Frost HJ, Ashby MF (1982) Deformation-Mechanism Maps: The Plasticity and Creep of Metals and Ceramics. Pergamon Press, Oxford, UK
27. Somekawa H, Hosokawa H, Watanabe H, Higashi K (2003) Mater Sci Eng A 339:328. doi:10.1016/S0921-5093(02)00127-2
28. del Valle JA, Carreño F, Ruano OA (2007) Scr Mater 57:829. doi:10.1016/j.scriptamat.2007.07.002
29. Langdon TG (2002) Metall. Mater Trans 33A:249
30. del Valle JA, Pérez-Prado MT, Ruano OA (2005) Metall. Mater Trans 36A:1427